

# Three-dimensional Taylor Green

## 1 Introduction

The Taylor-Green vortex at a Reynolds number of 1600 is a configuration commonly studied flow that captures elements of rudimental turbulence generation and decay [1], and serves as a case for a high-order workshop [2]. Unstructured, low-Mach numerical approaches were presented in [3] using a series of homogeneous topologies consisting of the following: Hex8, Hex27, Tet4, Pyramid5, and Wedge6.

The complete flow regime is marked by three phases that are described: Phase 1: viscous effects with small-scale laminar and organized structures are found; Phase 2: viscous (diffusion) effects dominating with accompanying stretching of vortex lines, and Phase 3: a break-up and is nearly isotropic in nature. Generally, for this simulation student, an explicit LES sub-grid stress model is omitted.

The initial condition for the three-dimensional flow field is as follows:

$$\begin{aligned} u_x &= u_o \sin\left(\frac{x}{L}\right) \cos\left(\frac{y}{L}\right) \cos\left(\frac{z}{L}\right), \\ u_y &= -u_o \cos\left(\frac{x}{L}\right) \sin\left(\frac{y}{L}\right) \cos\left(\frac{z}{L}\right), \\ u_z &= 0, \\ p &= p_o + \frac{\rho_o u_o^2}{16} \left( \cos\left(\frac{2x}{L}\right) + \cos\left(\frac{2y}{L}\right) \right) \left( \cos\left(\frac{2z}{L}\right) + 2 \right). \end{aligned} \quad (1)$$

The quantities of interest for this simulation study is the temporal evolution of the kinetic energy,  $E_k$ , that is integrated over the full domain at each time step. The energy-based dissipation rate given by  $\epsilon_1 = -\frac{dE_k}{dt}$ . The integrated enstrophy,  $\zeta$  is defined by (in a low-Mach flow),  $\epsilon_2 = \frac{2\mu}{\rho_o} \zeta$ , where,

$$\zeta = \frac{1}{\rho_o V} \int_{\Omega} \frac{1}{2} \rho \omega_k \omega_k d\Omega. \quad (2)$$

For more details, see [4].

## 2 Domain

The simulation is run in a periodic square box of  $-\pi L \leq x, y, z \leq \pi L$  with  $L$  equal to unity. The simulation is allowed to evolve from this initial condition

over 20 characteristic convection time scales (defined by  $t_c = \frac{L}{u_o}$ ). For this configuration, peak dissipation occurs at approximately  $8t_c$ .

## 2.1 Simulation Specification and Sample Results

A sample Q-criterion set of images for a Taylor-Green Re 1600 image appearing in [3] is shown in Figure 1, while the set of converged results in this same paper are shown in Figure 2.

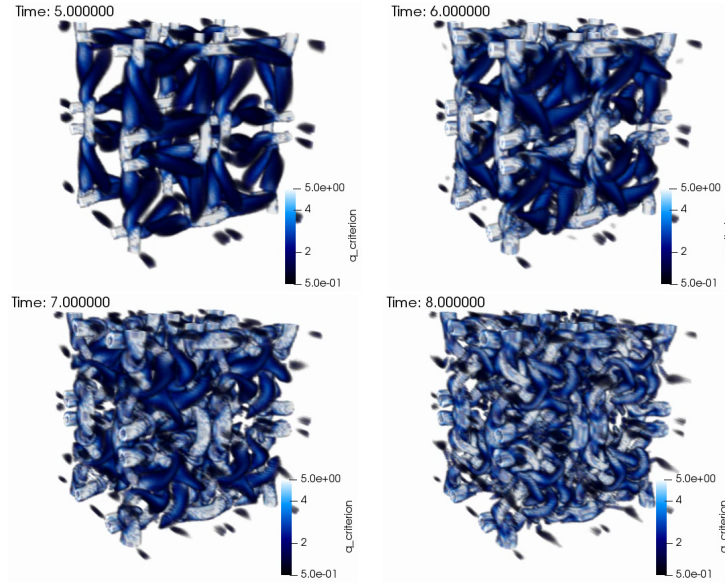


Figure 1: Three-dimensional Q-criterion volume rendered Taylor-Green representative time series at 5, 6, 7, and 8 seconds.

## 2.2 Meshes

The set of meshes provided in the mesh directory are as follows:

3d\_hex8\_taylor\_green\_0p2.g, 3d\_tet4\_taylor\_green\_0p2.g, and 3d\_tet4\_taylor\_green\_0p4.g. The mesh named “0p4” uses a 0.4 element length scale that can be useful for trouble shooting the monolithic implementation. Note that most peer-reviewed results appearing in the open literature exercise meshes that, even for a coarsest mesh spacing reported, are far more refined than the meshes provided in this study. However, the prime motivation for this exercise is to learn more about fully implicit solver approaches in the low-Mach limit.

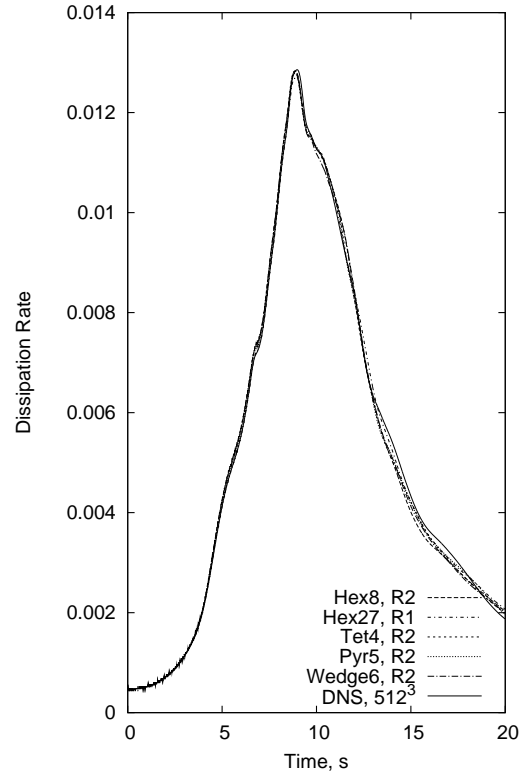


Figure 2: Turbulence dissipation rate temporal plot for the series of mesh refinements in [3]. In this study, the baseline (R0) Hex8 mesh spacing of  $\frac{2\pi}{100L}$ , i.e.,  $100^3$  elements was used.

### 3 Equation Set

The variable-density low-Mach equation set is defined by the continuity and momentum equation, here shown in integral form,

$$\int \frac{\partial \rho}{\partial t} dV + \int \rho \hat{u}_j n_j dS = 0, \quad (3)$$

$$\int \frac{\partial \rho u_i}{\partial t} dV + \int \rho \hat{u}_j u_i n_j dS - \int 2\mu S_{ij}^* n_j dS = \int P \delta_{ij} n_j dS \quad (4)$$

In the above equation,  $\rho$  is the fluid density and  $u_i$  is the fluid velocity, while the traceless rate-of-strain tensor is defined as

$$S_{ij}^* = S_{ij} - \frac{1}{3} \delta_{ij} S_{kk} = S_{ij} - \frac{1}{3} \frac{\partial u_k}{\partial x_k} \delta_{ij}.$$

In a low-Mach flow, the above pressure,  $P$ , is the perturbation about the thermodynamic pressure,  $P^{th}$ . We also note that the form shown above includes pressure stabilization embedded in the special velocity,  $\hat{u}_j$ , whose form can be written as,

$$\rho \hat{u}_j = \rho u_j - \frac{\Delta t}{\gamma_1} \left( \frac{\partial P}{\partial x_j} - G_j P \right), \quad (5)$$

where the projected nodal gradient,  $G_j P$  is obtained though the following equation:

$$\int G_j P dV - \int P n_j dS = 0. \quad (6)$$

When using higher-order approaches, and to retain design-order accuracy,  $G_j P$  must be computed using the consistent mass matrix, while using mass-lumping, yields,

$$G_j P = \frac{\int P n_j dS}{\int dV}. \quad (7)$$

### 4 Discussion Points

There are several interesting activities associated with this sample case including the points captured below.

- Document the appropriate equations for this conceptual model problem. Feel free to enforce the incompressible constraint since this approach simplifies the momentum time and viscous term.

- Run the pressure projection input file (modified to run at least to 20 seconds), while post-processing the integrated kinetic energy and dissipation plots. For the reference DNS of [2], see the “data” directory.
- Implement an interior monolithic momentum and continuity kernel that captures the equation contributions identified in the above first step. As a hint, this kernel should look very much like a combination of the segregated continuity (ContinuityAdvElemKernel) and momentum (MomentumAdvDiffElemKernel and MomentumMassElemKernel) classes, while noting that the total size of the system is  $nDim + 1$ . In the LowMachMonolithicEquationSystem class, note that a single contribution is expected by the name of: `uvwp_time_advection_diffusion` (a consistent-mass kernel) or `uvwp_lumped_time_advection_diffusion` (a lumped-mass kernel). Explore the usage of pressure stabilization in the momentum mass flow rate expression, in addition to using the “old” values for the momentum and projected nodal pressure gradient field. You may also explore other forms of the advection form, although do not worry about implementing a limited upwind operator.
- Compare and contrast the simulation timings between the pressure projection and monolithic implementation.
- *Optional* As time permits, perform any mesh refinement and comment on the sensitivity of the QoIs.
- *Optional* Perform any appropriate code verification using, for example, the convecting Taylor Vortex analytical solution on a periodic domain using your newly coded monolithic implementation.

## References

- [1] G. I. Taylor and A. E. Green. Mechanism of the production of small eddies from large ones. *Proc. Roy. Soc. Lond.*, 158:499–521, 1937.
- [2] K. Hillewaert. First international workshop on high-order cfd methods. Number AIAA 2012 in 50th Aerospace Sciences Meeting and Exhibit, Aerospace Sciences Meeting, Nashville, TN, Jan. 7–8, 2012, AIAA, Washington, D.C., 2012. AIAA.
- [3] S. Domino, P. Sakievich, and M. Barone. An assessment of atypical mesh topologies for low-Mach large-eddy simulation. *Comp. Fluids*, 179:655–669, 2019.
- [4] J. R. Bull and A. Jameson. Simulation of the taylor–green vortex using high-order flux reconstruction schemes. *AIAA Journal*, 53(9):2750–2761, 2015.